Integrated Source of Spectrally Filtered Correlated Photons for Large-Scale Quantum Photonic Systems

Nicholas C. Harris,[1] Davide Grassani,[2] Angelica Simbula,[2] Mihir Pant,[1] Matteo Galli,[2] Tom Baehr-Jones,[3] Michael Hochberg,[3] Dirk Englund,[1] Daniele Bajoni,[4] and Christophe Galland[5]

[1]*Department of Electrical Engineering and Computer Science, Massachusetts Institute of Technology, 77 Massachusetts Avenue, Cambridge, Massachusetts 02139, USA*
[2]*Dipartimento di Fisica, Università degli Studi di Pavia, via Bassi 6, 27100 Pavia, Italy*
[3]*Coriant Advanced Technology Group, 1415 West Diehl Road, Naperville, Illinois 60563, USA*
[4]*Dipartimento di Ingegneria Industriale e dell'Informazione, Università degli Studi di Pavia, via Ferrata 1, 27100 Pavia, Italy*
[5]*Ecole Polytechnique Fédérale de Lausanne, 1015 Lausanne, Switzerland*

(Received 30 September 2014; published 19 December 2014)

We demonstrate the generation of quantum-correlated photon pairs combined with the spectral filtering of the pump field by more than 95 dB on a single silicon chip using electrically tunable ring resonators and passive Bragg reflectors. Moreover, we perform the demultiplexing and routing of signal and idler photons after transferring them via an optical fiber to a second identical chip. Nonclassical two-photon temporal correlations with a coincidence-to-accidental ratio of 50 are measured without further off-chip filtering. Our system, fabricated with high yield and reproducibility in a CMOS-compatible process, paves the way toward large-scale quantum photonic circuits by allowing sources and detectors of single photons to be integrated on the same chip.

DOI: 10.1103/PhysRevX.4.041047 Subject Areas: Optics, Photonics, Quantum Information

I. INTRODUCTION

Integrated photonic circuits have emerged as a promising platform for quantum information processing [1–3]. The most mature technology for scalable photonic circuits is based on CMOS-compatible materials such as silicon, silicon nitride, and silica. In these platforms, pairs of quantum-correlated photons produced by spontaneous four-wave mixing (SFWM) are an essential resource for quantum technologies including linear quantum optics experiments [4–7] and quantum sensing [8].

Photon-pair generation via SFWM involves pumping a nonlinear medium (such as silicon) with a strong laser field, which must subsequently be filtered to isolate the much weaker signal and idler fields and perform single-photon detection. However, for scalable integration into quantum optics circuits, two challenges must be solved: the on-chip rejection of the pump field and spectral demultiplexing. In particular, and despite very recent attempts [9,10], the filtering of the pump field, which requires an extinction on the order of approximately 100 dB, has never been achieved without using off-chip filters.

Here, we demonstrate the generation of time-correlated photon pairs in a silicon microring with on-chip rejection of the pump field. We also perform chip-to-chip transfer of the photon pairs via an optical fiber, elimination of the pump field, and signal and idler demultiplexing before off-chip single-photon detection. A set of four single-photon sources with pump rejection and demultiplexing circuitry in a 3.3-mm^2 area is fabricated in a standard CMOS silicon-photonics process featuring high yield and reproducibility.

The source components are shown in Fig. 1. Photon-pair generation takes place in an electrically tunable ring resonator [11–15] via SFWM [16–21] [Figs. 1(a) and 1(b)]. A first stage of pump rejection by approximately 65 dB is achieved using a notch filter implemented by a 2.576-mm-long distributed Bragg reflector (DBR) consisting of a corrugated waveguide [Fig. 1(c)] [22]. Signal and idler photon demultiplexing is performed using add-drop microring resonators as shown in [Fig. 1(d)]. In a first experiment performed on a single chip [chip *A*, Fig. 1(e)], two thermally tunable add-drop ring resonators are used to filter the remaining pump light, thereby totaling close to a 100-dB extinction ratio. At the output of chip *A*, the pump power is less than $1/10$ of the combined signal and idler fields.

In a second experiment, we transfer the photon pairs from chip *A* via a silica-fiber connection to a similar system on a second chip [chip *B*, Fig. 1(f)] in which we filter any residual pump with the DBR and use the add-drop rings to demultiplex the signal and idler photons [Fig. 1(d)]. These photon pairs are then routed to different waveguides before detection with off-chip superconducting-nanowire single-photon detectors (SNSPDs) and time-correlation

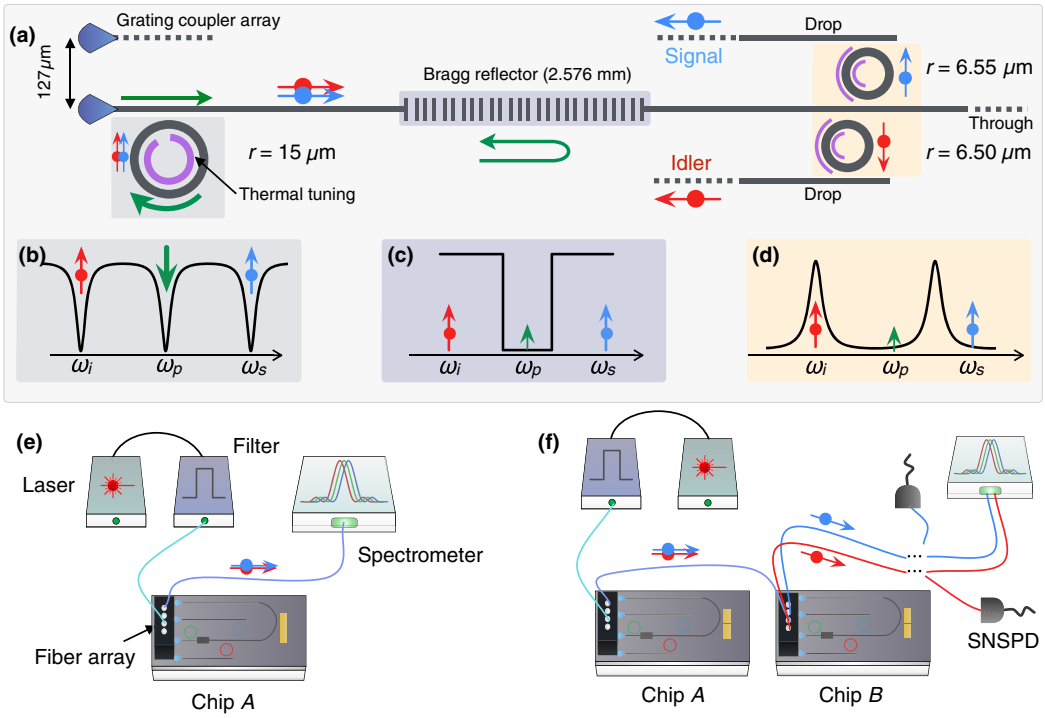

FIG. 1. (a) Schematic layout of the photonic integrated circuit composed of a high-Q thermally tunable ring for efficient pair generation by spontaneous four-wave mixing, followed by a DBR for pump rejection and the add-drop ring-resonator filters for the demultiplexing of signal and idler photons. Convenient optical coupling to a single-mode polarization-maintaining fiber array is achieved via focusing grating couplers separated by a 127-μm pitch. (b) Schematic transmission spectrum of the first ring around the pump wavelength ω_p. When one of the ring resonances is tuned to the laser at ω_p, signal and idler photons are produced in correlated pairs at neighboring resonance wavelengths ω_s and ω_i, respectively. (Pairs are also generated at wavelengths spaced by multiple free spectral ranges.) (c) Schematic transmission spectrum of the DBR with the stop band overlapping with the pump wavelength ω_p. (d) Add-drop filter spectrum tuned to route idler photons to the drop port. (e) First experimental setup: single-chip pump rejection. The add-drop rings are both tuned on resonance with the pump. Light is collected from the common throughport. (f) Second experimental setup (see Supplemental Fig. 4 for a photograph [23]): Correlated photon pairs generated in chip A are sent via a fiber to chip B where further pump rejection and signal or idler demultiplexing are performed before spectral characterization or coincidence measurements with off-chip SNSPDs.

measurements. The coincidence-to-accidental ratio exceeds 50 for a continuous pump power of approximately 0.3 mW, confirming successful on-chip full suppression of the pump light and demultiplexing of signal and idler photons.

Together with previous realizations of (i) integrated laser sources [24–30], (ii) on-chip sources of quantum states of light [17,19–21,31–40], (iii) on-chip quantum-state manipulation [1,6,41–46], and (iv) on-chip single-photon detection [47–52], our work addresses the challenge of integrating single-photon sources and detectors on the same chip. Our results highlight the promises of CMOS photonics for emerging quantum technologies such as quantum key distribution [53–63], quantum simulations and random walks [4,46,64–68], and possibly quantum computation [69–74].

II. SYSTEM DESIGN

Pair generation.—As a source of photon pairs, we employ a silicon ring resonator evanescently coupled to the input waveguide. (See the Supplemental Material for further details [23].) Field enhancement inside the resonator results in an increased generation of correlated photon pairs (with respect to non-cavity-based generation methods) [17,19,20,75] when the pump (ω_p), signal (ω_s), and idler (ω_i) frequencies match a triplet of ring resonances fulfilling $\omega_i + \omega_s = 2\omega_p$. For a given pump power, the flux of photon pairs produced by SFWM is proportional to the ratio Q^3/R^2, where Q is the quality factor and R the radius of the ring [18,75]. Based on these considerations, we design the pair-generation ring [Fig. 1(b)] with a radius of 15 μm, leading to an expected free spectral range of 6 nm. To allow for spectral tunability without compromising on the quality factor, we add an inner semiring of doped silicon to form a resistive heater.

Pump rejection.—We expect the ratio between the pump power inside the ring resonator and the generated signal and idler beams to be of the order of 10^9 to 10^{10}, and thus, pump rejection of approximately 100 dB is required. Achieving pump-rejection levels on this order constitutes

the most demanding requirement for the system. The center-reflection wavelength of the DBR notch filter [22] is designed to be $\lambda_0 = 2n_{\text{eff}}\Lambda \sim 1536$ nm, as defined by the Bragg period $\Lambda = 320$ nm and the effective index $n_{\text{eff}} \sim 2.4$. We design the width of the reflection band to be smaller than the generation-ring free spectral range [see Fig. 1(c)] but large enough to avoid the need for delicate spectral tuning. This width depends on the refractive-index contrast of the grating (given here by the amplitude of the sidewall corrugation). A 60-nm modulation of the waveguide width is found to yield spectral linewidths of 1–2 nm. The transmission in the reflection band drops exponentially with the number of grating periods. While developing the DBR device, we measure the extinction ratio of approximately 20–25 dB for devices with 2000 periods—prompting the choice of 8000 periods for the system presented here. To reduce the total footprint, we introduce a bend halfway in the DBR waveguide, which leads to weak Fabry-Perot effects.

Signal or idler demultiplexing.—The add-drop ring resonators used to filter the remaining pump and/or route signal and idler photons are designed to cause minimal excess loss and to be thermally tunable by an embedded resistive heater formed by doped silicon regions contacted to the metal interconnect layer. To minimize losses due to free-carrier absorption, we use a low dopant concentration in the waveguide region overlapping with the optical mode. To maximize the collection efficiency in the drop port (where single photons are routed), we design the device to be overcoupled.

Optical in or out coupling.—An array of optimized nonuniform focusing grating couplers [76] offers a convenient and efficient (4-dB insertion loss; see the Supplemental Material [23]) way to couple light between a single-mode fiber array and the silicon waveguides. Moreover, the large-mode field diameter of the grating couplers (10 μm) enables stable optical coupling.

III. FABRICATION

The system is fabricated in a CMOS-compatible foundry service (OpSIS) with 248-nm lithography on an 8-in silicon-on-insulator wafer with a 220-nm-thick epitaxial silicon layer (bulk refractive index $n_{\text{Si}} = 3.48$ at 1550 nm)

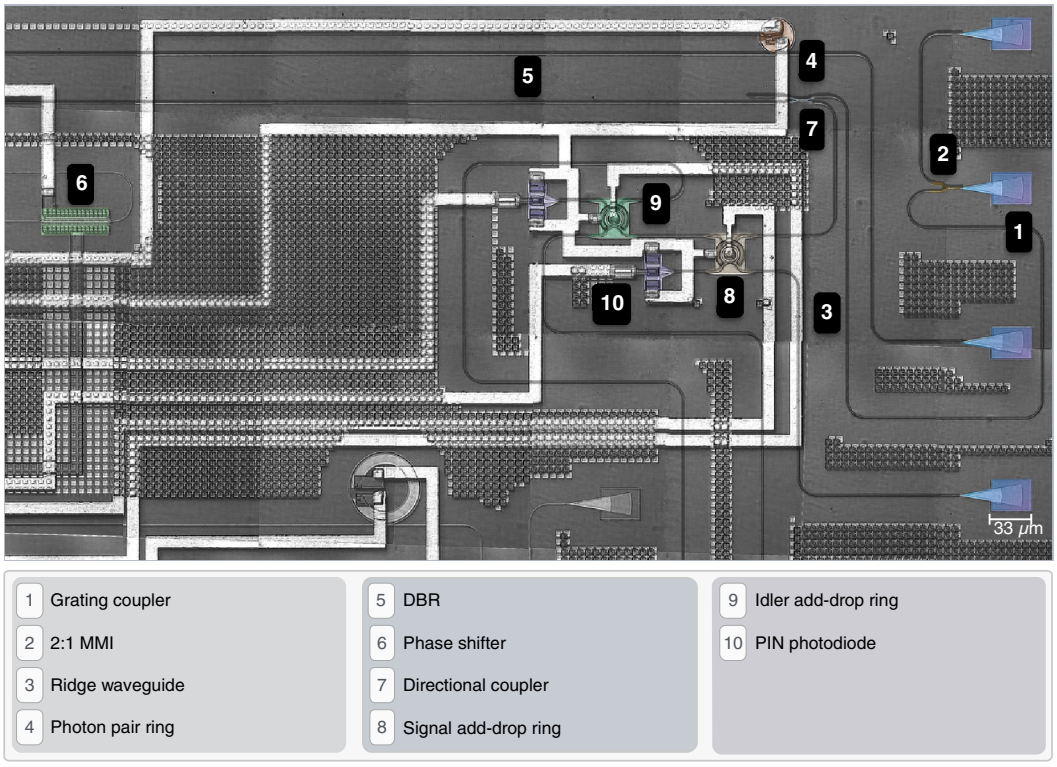

FIG. 2. Optical micrograph of the single-photon source (one of four on the chip in an area of 2.4 by 1.36 mm^2). Two grating couplers are not shown (see the Supplemental Material [23]). (1) Grating couplers used to couple (collect) light to (from) the system are shown on the right. The input light is split by (2) a 2:1 multimode interferometer for optical alignment. Pump light is then routed via (3) a 500-by-220-nm ridge waveguide to (4) the pair-generation ring. The pump is removed with (5) the DBR, which is divided into two sections [(6) Fabry-Perot resonances due to the division can be controlled with the thermo-optic phase shifter [78]]. The multiplexed signal- and idler-photon combs are then split off for spectral monitoring at (7) the directional coupler before demultiplexing and/or further filtering with the (8) signal and (9) idler add-drop rings. (10) The p-doped/intrinsic/n-doped germanium photodiodes were not used during the experiment; however, they could be used to monitor the add-drop ring alignment.

on top of 2 μm of buried oxide and covered by 2 μm of oxide cladding (bulk index $n_{SiO_2} = 1.46$). The grating couplers and rib waveguides are defined by 60- and 130-nm-deep anisotropic dry etching, respectively. A final etch step down to the buried oxide is used to pattern the 500-nm-wide by 220-nm-tall ridge waveguides designed to be single mode in the 1500–1600-nm wavelength range. (These waveguides are used for routing throughout the chip.) *N*-type doping of the tunable ring resonators is realized by phosphorous implantation on the exposed silicon before oxide cladding. Dopants are activated by a rapid thermal anneal at 1030 °C for 5 s. The back end of the line consists of two levels of aluminum interconnects contacted by aluminum vias. Further technical details on the process can be found in Ref. [77]. A micrograph of the chip area containing four similar complete systems is reproduced in Fig. 2.

IV. SINGLE-CHIP PUMP REJECTION

A high-resolution transmission spectrum of the complete system is shown in Fig. 3(a). This spectrum is acquired using a tunable laser and a high dynamic-range power meter. The dip around 1525 nm is due to the DBR and is detailed in the high-resolution spectrum of Fig. 3(b). Note that weak Fabry-Perot effects in the spectrum are the result of the waveguide-bend section between the sections of DBR. In control experiments, we observe that some of the laser light is directly coupled from the input to the output fibers—without passing through the waveguides—by scattering and reflections in the SiO_2 cladding and Si substrate. As a result, the measured rejection of the DBR is reduced with respect to the expected value of 80–100 dB to approximately 65 dB with an insertion loss of approximately 3 dB. Weak Fabry-Perot resonances are visible near the red edge of the stop band due to the cavity formed by the bend separating the two halves of the DBR. Better rejection could be achieved in a future implementation by having a larger spatial separation between the input and output grating couplers to avoid collecting scattered pump light.

The wider Lorentzian resonances in the spectra are due to the two final add-drop rings, with a quality factor (Q) of approximately 4×10^3 and an insertion loss of approximately 1.5 dB. The narrow Lorentzian resonances are due to the photon-pair-generation ring, with a Q of approximately 4×10^4 (corresponding to a photon lifetime of about 30 ps). Such a high quality factor is of fundamental importance in providing a sufficiently high generation rate at an easily achievable mW pump-power level [18] and for ensuring emission of quantum states with narrow bandwidth [79].

The spectrum is attenuated by approximately 1 dB due to a directional coupler designed for monitoring of the system

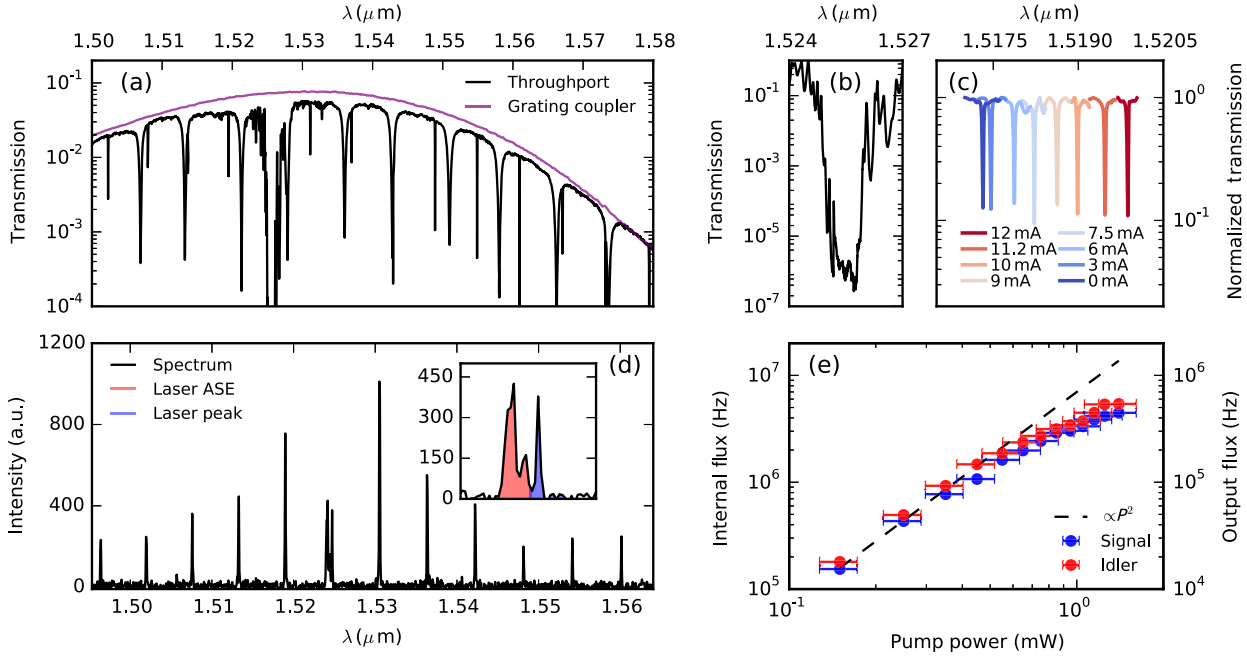

FIG. 3. Single-chip pump-rejection data set. (a) Logarithmic plot of the transmission spectrum measured at the throughport of chip *A* after propagation through the complete system. The upper curve is the transmission of a grating-coupler loop. (b) Higher-resolution spectrum around the DBR stop band. (c) Spectrum of the pair-generation ring around the signal wavelength under increasing current driving the resistive heater. 11.2 mA is the value used in the coincidence measurements presented in Fig. 4. (e) Dependence of the SFWM generation rate for the signal (blue circles) and idler (red circles) photons as a function of on-chip pump power. (The dashed line is a guide to the eye proportional to P^2_{pump}.) The right-hand scale is the off-chip count rate after correction for the CCD efficiency. The left-hand scale is the estimated internal generation rate inside the ring resonator.

under operation. The sinusoidal envelope is due to the grating-coupler spectral response (measured insertion loss of 5 dB) and depends on the tilt angle of the input and output fibers. The transmission from a grating-coupler loop is also shown in Fig. 3(a) for comparison. The fiber-array tilt angle is chosen to optimize the coupling around the pump wavelength (approximately 1525 nm).

The setup for the first experiment is shown in Fig. 1(e). The external pump laser is cleaned through a tunable bandpass filter to suppress the sidebands below the expected SFWM yield. It is coupled to chip *A* via an eight-port fiber array aligned with the focusing grating couplers [76]. The pump laser and the generation ring are tuned in resonance with each other so that their wavelengths lie within the DBR stop band [Fig. 3(a)]. Inside the ring, signal and idler photons are spontaneously generated in pairs at resonance frequencies symmetrically detuned from the pump. The pump light is first rejected by the DBR [Fig. 3(b)] and then filtered by the two add-drop filters, which are tuned on resonance with the pump wavelength.

The spectrum of the light collected at the common throughport, for a coupled laser power of 1 mW, is plotted in Fig. 3(d). Residual light from the pump is still visible around 1524.7 nm, but it is greatly reduced. We estimate a total extinction ratio of about 95–100 dB. Notice that part of the amplified spontaneous emission (ASE) of the laser is still visible in our spectrum [inset of Fig. 3(d)]. The remaining ASE could be suppressed by using a filter with narrower bandwidth (instead of 0.15 nm here) to clean the laser line (which could easily be implemented on chip, too). The sum of the intensities in the first five signal peaks (respectively, in the first five idler peaks) is a factor of 8 (respectively, 10) larger than the residual laser. Remaining pump photons follow Poissonian statistics and are not correlated in time; therefore, this level of suppression is already sufficient for many quantum optical experiments [80] like heralding of single photons or entanglement generation.

The dependence of signal and idler intensities on the pump power is plotted in Fig. 3(e). Both intensities follow the quadratic dependence on pump power expected for SFWM, and around 1-mW on-chip pump-power saturation due to two-photon absorption [15] becomes visible. To measure the photon rate at the sample output, we have calibrated our CCD camera using a high-sensitivity power meter. The internal generation rate, on the order of several MHz, is then estimated by subtracting the losses on the path from the output to the generating ring to the spectrometer.

V. CHIP-TO-CHIP TRANSFER, DEMULTIPLEXING, AND CORRELATION MEASUREMENTS

In a second experiment [Fig. 1(f)], we generate photon pairs and filter the pump beam on chip *A* using the generation-microring resonator and DBR. The signal and the idler demultiplexing rings are both tuned out of resonance from pump, signal, and idler wavelengths, so that they transmit all of them to the drop port. The output of chip *A* is transferred to a similar system on chip *B* via an optical fiber. The DBR of chip *B* is tuned on resonance with the pump wavelength (proving an additional approximately 65 dB of pump isolation) by temperature control of the full chip [see Supplemental Fig. 3(d) [23]], and the add-drop filters on chip *B* are tuned individually to perform demultiplexing of the signal and idler photons [see Fig. 1(d)] while further eliminating residual pump photons. The total pump isolation in this experiment is approximately 150 dB. The total loss for the signal (idler) photons collected on the first (second) SNSPD is 36.14 dB (39.14 dB), as shown in Table I.

Figures 4(a) and 4(b) show the spectrum of the common throughport on chip *B* (a) before and (b) after tuning the add-drop rings. It demonstrates (i) the efficient generation of signal and idler photons by SFWM at the resonance wavelengths of the pair-generation ring and (ii) the almost complete rejection of the pump beam (missing central peak around 1525 nm). The pronounced decrease in the intensity of the generated fields moving away from the pump wavelength is due to the spectral response of input and output grating couplers [see Fig. 3(a)].

As desired, the signal and idler emission lines are not visible in the throughport after tuning. The corresponding spectra from the signal and idler throughports are shown in Figs. 4(c) and 4(d), respectively. Each resonance is appropriately routed to an individual drop port, and no trace of the pump or of the opposite resonance is visible. Our data indicate the first realization of on-chip SFWM with pump

TABLE I. Summary of the losses for signal and idler photons throughout the optical path for the chip-to-chip transfer experiment. The intrinsic grating-coupler insertion loss and ridge waveguide-propagation loss are 4.4 ± 0.2 dB and 2.4 ± 0.3 dB/cm, respectively (as reported in Ref. [77]).

(Chip) Cause	Signal (dB)	Idler (dB)	Total (dB)
(*A*) DBR	3	3	6
(*A*) 1:2 multi-mode interferometer [81]	0.28	0.28	0.56
(*A*) Phase shifter [78]	0.23	0.23	0.46
(*A*) Monitoring tap	1	1	2
(*A*) Output grating coupler	5	5	10
(*A*) Waveguide loss [77]	0.31	0.31	0.62
(*B*) Input grating coupler	5	5	10
(*B*) DBR	3	3	6
(*B*) 1:2 multi-mode interferometer [81]	0.28	0.28	0.56
(*B*) Phase shifter [78]	0.23	0.23	0.46
(*B*) Monitoring tap	1	1	2
(*B*) Add-drop filter	1.5	1.5	3
(*B*) Waveguide loss [77]	0.31	0.31	0.62
(*B*) Output grating coupler	5	5	10
Detection efficiency	10	13	23
Total	36.14	39.14	75.28

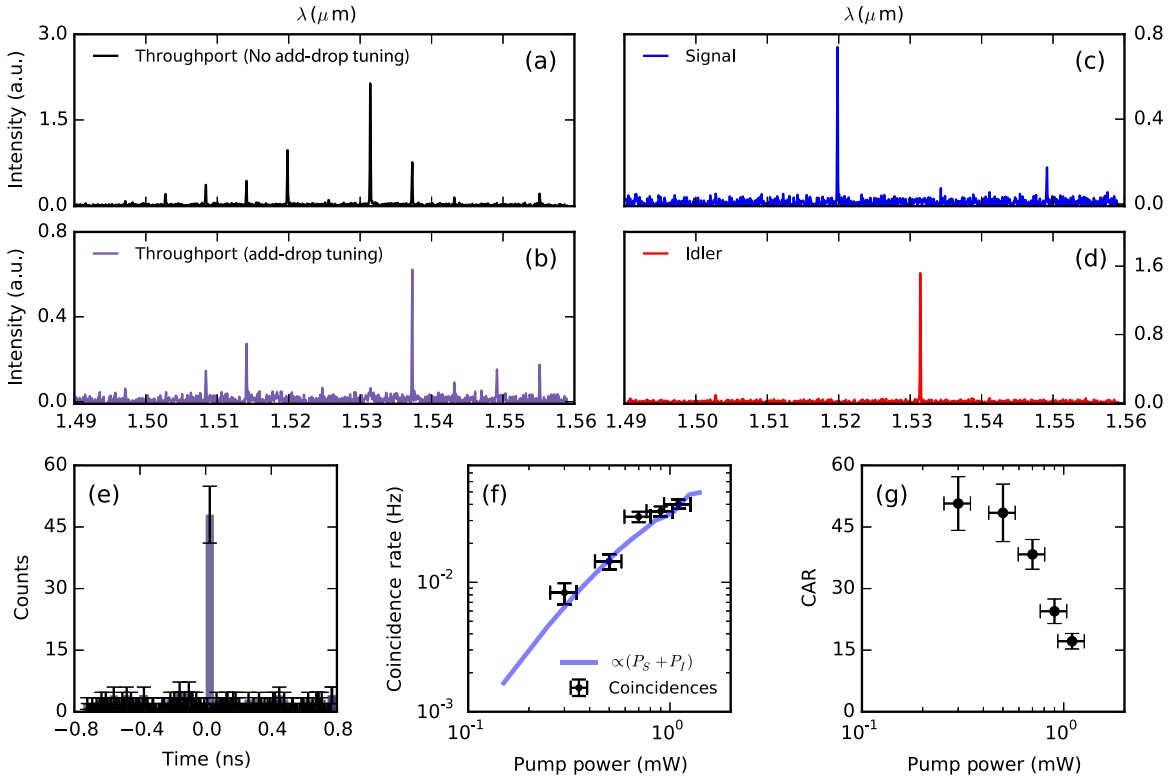

FIG. 4. Chip-to-chip photon-pair transfer data set. (a) SFWM spectra as observed at the throughport of chip *B* without tuning the add-drop ring filters (black line) and (b) with add-drop filters tuned to the signal and idler wavelengths (purple line). (c),(d) The SFWM spectra as observed at the idler (red line) and signal (blue line) drop ports of chip *B*, respectively, when the add-drop filters are tuned as in (b). In all panels, $P_{\text{pump}} = 0.5$ mW in chip *A*. (e) Coincidence histogram between the signal and idler ports of chip *B* for a pump power $P_{\text{pump}} = 0.5$ mW in chip *A*. The total acquisition time is 50 min. (f) Dependence of the coincidence rate on the pump power. The dashed line is proportional to the measured signal and idler combined intensities. (g) Pump-power dependence of the coincidental-to-accidental ratio (CAR).

rejection and signal or idler demultiplexing achieved without any off-chip postfiltering elements.

We measure two-photon time correlations between the two drop-port outputs of chip *B* using two SNSPDs with 10% and 5% quantum efficiency, without external filters. The bias current is set to have dark-count rates of the order of 300 Hz. An example of coincidence measurement is shown in Fig. 4(e). A clear coincidence peak is visible at zero time delay. Accidental events outside the central peak are mainly caused by coincidences between dark counts and the detection of only one photon in a pair.

The dependence of the coincidence rate after chip *B* on the pump power inside chip *A* is shown in Fig. 4(f). The dependence closely follows the combined signal and idler emission rates, reported in the figure after rescaling for clarity. The total losses on the coincidences are given from the product of the total losses on both channels, from the generating ring to the detectors, amounting to a total of 75.28 dB (see the discussion in the Supplemental Material [23]). Finally, in Fig. 4(g), we show the coincidence-to-accidental ratio [19,80,82] as a function of the pump power in chip *A*. A value of 50 ± 6—far above the classical limit of 2 and allowing for high-fidelity preparation of entangled-photon pairs or heralded single photons—is achieved under 0.3-mW pump power.

VI. DISCUSSION AND OUTLOOK

Quantum information processing based on linear-optics quantum computing will require efficient single-photon sources and detectors as well as feed-forward operations [71,83]. The potential for multiplexing the emission of parametric single-photon sources [84,85] could enable high-efficiency state preparation for quantum computation. The system presented here permits the integration of single-photon sources and detectors on a single chip, providing a means of achieving large-scale systems for linear-optics quantum computing.

Boson sampling has received significant attention [4,64,67] for its promise to demonstrate the first example of quantum speedup over the fastest known classical algorithm. Leveraging the reproducibility and high yield of integrated photonics, our system could be tiled to enable boson sampling with many sources. The signal photon could be used as a herald for the idler photon (or vice versa) in a scheme such as scattershot boson sampling [86] where the measurements are

postselected based on the number of photons that enter the quantum random walk simultaneously. The dimension of the input state can thereby be scaled up in a probabilistic scheme.

Finally, it has been shown that the type of SFWM source used here produces time-energy entangled-photon pairs [87]. These time-energy entangled-photon pairs generated with our architecture could enable fully integrated quantum-key-distribution emitters and receivers based on time-energy entanglement protocols [63,88]. The geometry of nanoscale silicon waveguides can be engineered to achieve both normal and anomalous dispersion, as necessary to realize this protocol.

VII. CONCLUSION

We have demonstrated, for the first time in a monolithic, tunable silicon-photonic chip, the generation of quantum-correlated photon pairs in an electrically tunable ring resonator and the rejection of the pump field by more than 95 dB using a Bragg reflector and tunable ring filters—enabling the integration of single-photon sources and single-photon detectors on chip [47,48]. Moreover, we achieved complete pump rejection and spatial demultiplexing of signal and idler photons by employing two identical chips connected by an optical fiber link. With no additional off-chip filtering, we measured signal-idler temporal correlations with a coincidence-to-accidental ratio of 50 at the output of the demultiplexing chip, confirming their nonclassical nature. Each source, whose total footprint is less than 1 mm^2, is fabricated using a conventional CMOS-compatible photonic process featuring high yield, reproducibility, dense integration, and scalability. By eliminating the need for the last off-chip components, our result opens new possibilities for large-scale quantum photonic systems with on-chip single- and entangled-photon sources.

ACKNOWLEDGMENTS

N. C. H. acknowledges that this material is based upon work supported by the National Science Foundation Graduate Research Fellowship under Grant No. 1122374. This work was supported in part under a grant from the Air Force Research Laboratory (AFRL/RITA), Grant No. FA8750-14-2-0120. Any opinions, findings, and conclusions or recommendations expressed in this material are those of the author(s) and do not necessarily reflect the views of the AFRL. The authors are also grateful for the support of Portage Bay Photonics and of Gernot Pomrenke of the AFOSR, who has supported the broader research program of Optoelectronic Systems Integration in Silicon over multiple programs. D. G., D. B., and M. G. acknowledge support from Ministero dell'Istruzione, Università e Ricerca through the Fondo per gli Investimenti della Ricerca di Base "Futuro in Ricerca" project RBFR08XMVY, from the foundation Alma Mater Ticinensis, and by Fondazione Cariplo through Project No. 2010-0523 Nanophotonics for thin-film photovoltaics. C. G. is supported by an *Ambizione* Fellowship from the Swiss National Science Foundation. C. G. thanks Sébastien Tanzilli for valuable comments and discussions.

N. C. H. and D. G. contributed equally to this work.

[1] J. W. Silverstone, D. Bonneau, K. Ohira, N. Suzuki, H. Yoshida, N. Iizuka, M. Ezaki, C. M. Natarajan, M. G. Tanner, R. H. Hadfield, V. Zwiller, G. D. Marshall, J. G. Rarity, J. L. O'Brien, and M. G. Thompson, *On-Chip Quantum Interference between Silicon Photon-Pair Sources*, Nat. Photonics **8**, 104 (2014).

[2] M. J. Collins, C. Xiong, I. H. Rey, T. D. Vo, J. He, S. Shahnia, C. Reardon, T. F. Krauss, M. J. Steel, A. S. Clark, and B. J. Eggleton, *Integrated Spatial Multiplexing of Heralded Single-Photon Sources*, Nat. Commun. **4**, 1 (2013).

[3] S. Tanzilli, A. Martin, F. Kaiser, M. P. De Micheli, O. Alibart, and D. B. Ostrowsky, *On the Genesis and Evolution of Integrated Quantum Optics*, Laser Photonics Rev. **6**, 115 (2012).

[4] J. B. Spring, B. J. Metcalf, P. C. Humphreys, W. S. Kolthammer, X.-M. Jin, M. Barbieri, A. Datta, N. Thomas-Peter, N. K. Langford, D. Kundys, J. C. Gates, B. J. Smith, P. G. R. Smith, and I. A. Walmsley, *Boson Sampling on a Photonic Chip*, Science **339**, 798 (2013).

[5] A. Aspuru-Guzik and P. Walther, *Photonic Quantum Simulators*, Nat. Phys. **8**, 285 (2012).

[6] A. Politi, M. J. Cryan, J. G. Rarity, S. Yu, and Jeremy L. O'Brien, *Silica-on-Silicon Waveguide Quantum Circuits*, Science **320**, 646 (2008).

[7] A. Peruzzo, M. Lobino, J. C. F. Matthews, N. Matsuda, A. Politi, K. Poulios, X.-Q. Zhou, Y. Lahini, Nur Ismail, K. Wörhoff, Y. Bromberg, Y. Silberberg, M. G. Thompson, and J. L. O'Brien, *Quantum Walks of Correlated Photons*, Science **329**, 1500 (2010).

[8] J. C. F. Matthews, A. Politi, D. Bonneau, and J. L. O'Brien, *Heralding Two-Photon and Four-Photon Path Entanglement on a Chip*, Phys. Rev. Lett. **107**, 163602 (2011).

[9] J. R. Ong, R. Kumar, and S. Mookherjea, *Silicon Microring-Based Wavelength Converter with Integrated Pump and Signal Suppression*, Opt. Lett. **39**, 4439 (2014).

[10] N. Matsuda, P. Karkus, H. Nishi, T. Tsuchizawa, W. J. Munro, H. Takesue, and K. Yamada, *On-Chip Generation and Demultiplexing of Quantum Correlated Photons Using a Silicon-Silica Monolithic Photonic Integration Platform*, Opt. Express **22**, 22831 (2014).

[11] A. Yariv and P. Yeh, *Photonics* (Oxford University Press, New York, 2007).

[12] B. E. Little, J. S. Foresi, G. Steinmeyer, E. R. Thoen, S. T. Chu, H. A. Haus, E. P. Ippen, L. C. Kimerling, and W. Greene, *Ultra-compact* Si-SiO_2 *Microring Resonator Optical Channel Dropping Filters*, IEEE Photonics Technol. Lett. **10**, 549 (1998).

[13] W. Bogaerts, P. De Heyn, T. Van Vaerenbergh, K. De Vos, S. K. Selvaraja, T. Claes, P. Dumon, P. Bienstman, D. Van Thourhout, and R. Baets, *Silicon Microring Resonators*, Laser Photonics Rev. **6**, 47 (2012).

[14] V. R. Almeida, C. A. Barrios, R. R. Panepucci, and M. Lipson, *All-Optical Control of Light on a Silicon Chip*, Nature (London) **431**, 1081 (2004).

[15] Q. Xu and M. Lipson, *Carrier-Induced Optical Bistability in Silicon Ring Resonators*, Opt. Lett. **31**, 341 (2006).

[16] A. C. Turner, M. A. Foster, A. L. Gaeta, and M. Lipson, *Ultra-low Power Parametric Frequency Conversion in a Silicon Microring Resonator*, Opt. Express **16**, 4881 (2008).

[17] S. Clemmen, K. Phan Huy, W. Bogaerts, R. G. Baets, Ph. Emplit, and S. Massar, *Continuous Wave Photon Pair Generation in Silicon-on-Insulator Waveguides and Ring Resonators*, Opt. Express **17**, 16558 (2009).

[18] S. Azzini, D. Grassani, M. Galli, L. C. Andreani, M. Sorel, M. J. Strain, L. G. Helt, J. E. Sipe, M. Liscidini, and D. Bajoni, *From Classical Four-Wave Mixing to Parametric Fluorescence in Silicon Microring Resonators*, Opt. Lett. **37**, 3807 (2012).

[19] S. Azzini, D. Grassani, M. J. Strain, M. Sorel, L. G. Helt, J. E. Sipe, M. Liscidini, M. Galli, and D. Bajoni, *Ultra-low Power Generation of Twin Photons in a Compact Silicon Ring Resonator*, Opt. Express **20**, 23100 (2012).

[20] E. Engin, D. Bonneau, C. M. Natarajan, A. S. Clark, M. G. Tanner, R. H. Hadfield, S. N. Dorenbos, V. Zwiller, K. Ohira, N. Suzuki, H. Yoshida, N. Iizuka, M. Ezaki, J. L. O'Brien, and M. G. Thompson, *Photon Pair Generation in a Silicon Micro-ring Resonator with Reverse Bias Enhancement*, Opt. Express **21**, 27826 (2013).

[21] C. Reimer, L. Caspani, M. Clerici, M. Ferrera, M. Kues, M. Peccianti, A. Pasquazi, L. Razzari, B. E. Little, S. T. Chu, D. J. Moss, and R. Morandotti, *Integrated Frequency Comb Source of Heralded Single Photons*, Opt. Express **22**, 6535 (2014).

[22] X. Wang, W. Shi, H. Yun, S. Grist, N. A. F. Jaeger, and L. Chrostowski, *Narrow-Band Waveguide Bragg Gratings on SOI Wafers with CMOS-Compatible Fabrication Process*, Opt. Express **20**, 15547 (2012).

[23] See Supplemental Material at http://link.aps.org/supplemental/10.1103/PhysRevX.4.041047 for photon-pairgeneration ring details.

[24] A. W. Fang, H. Park, O. Cohen, R. Jones, M. J. Paniccia, and J. E. Bowers, *Electrically Pumped Hybrid AlGaInAs-Silicon Evanescent Laser*, Opt. Express **14**, 9203 (2006).

[25] S. Tanaka, S.-H. Jeong, S. Sekiguchi, T. Kurahashi, Y. Tanaka, and K. Morito, *High-Output-Power, Single-Wavelength Silicon Hybrid Laser Using Precise Flip-Chip Bonding Technology*, Opt. Express **20**, 28057 (2012).

[26] R. E. Camacho-Aguilera, Y. Cai, N. Patel, J. T. Bessette, M. Romagnoli, L. C. Kimerling, and J. Michel, *An Electrically Pumped Germanium Laser*, Opt. Express **20**, 11316 (2012).

[27] S. Keyvaninia, G. Roelkens, D. Van Thourhout, C. Jany, M. Lamponi, A. Le Liepvre, F. Lelarge, D. Make, G.-H. Duan, D. Bordel, and J.-M. Fedeli, *Demonstration of a Heterogeneously Integrated III-V/SOI Single Wavelength Tunable Laser*, Opt. Express **21**, 3784 (2013).

[28] T. Creazzo, E. Marchena, S. B. Krasulick, P. K. L. Yu, D. Van Orden, J. Y. Spann, C. C. Blivin, L. H., H. Cai, J. M. Dallesasse, R. J. Stone, and A. Mizrahi, *Integrated Tunable CMOS Laser*, Opt. Express **21**, 28048 (2013).

[29] J. H. Lee, I. Shubin, J. Yao, J. Bickford, Y. Luo, S. Lin, S. S. Djordjevic, H. D. Thacker, J. E. Cunningham, K. Raj, X. Zheng, and A. V. Krishnamoorthy, *High Power and Widely Tunable Si Hybrid External-Cavity Laser for Power Efficient Si Photonics WDM Links*, Opt. Express **22**, 7678 (2014).

[30] S. Yang, Y. Zhang, D. W. Grund, G. A. Ejzak, Y. Liu, A. Novack, D. Prather, A. E.-J. Lim, G.-Q. Lo, T. Baehr-Jones *et al.*, *A Single Adiabatic Microring-Based Laser in 220 nm Silicon-on-Insulator*, Opt. Express **22**, 1172 (2014).

[31] J. E. Sharping, K. F. Lee, M. A. Foster, A. C. Turner, B. S. Schmidt, M. Lipson, A. L. Gaeta, and P. Kumar, *Generation of Correlated Photons in Nanoscale Silicon Waveguides*, Opt. Express **14**, 12388 (2006).

[32] L. Lanco, S. Ducci, J.-P. Likforman, X. Marcadet, J. A. W. van Houwelingen, H. Zbinden, G. Leo, and V. Berger, *Semiconductor Waveguide Source of Counterpropagating Twin Photons*, Phys. Rev. Lett. **97**, 173901 (2006).

[33] H. Takesue, Y. Tokura, H. Fukuda, T. Tsuchizawa, T. Watanabe, K. Yamada, and S.-i. Itabashi, *Entanglement Generation Using Silicon Wire Waveguide*, Appl. Phys. Lett. **91**, 201108 (2007).

[34] K.-i. Harada, H. Takesue, H. Fukuda, T. Tsuchizawa, T. Watanabe, K. Yamada, Y. Tokura, and S.-i. Itabashi, *Generation of High-Purity Entangled Photon Pairs Using Silicon Wire Waveguide*, Opt. Express **16**, 20368 (2008).

[35] C. Xiong, C. Monat, A. S. Clark, C. Grillet, G. D. Marshall, M. J. Steel, J. Li, L. O'Faolain, T. F. Krauss, J. G. Rarity, and B. J. Eggleton, *Slow-Light Enhanced Correlated Photon Pair Generation in a Silicon Photonic Crystal Waveguide*, Opt. Lett. **36**, 3413 (2011).

[36] N. Matsuda, H. Le Jeannic, H. Fukuda, T. Tsuchizawa, W. J. Munro, K. Shimizu, K. Yamada, Y. Tokura, and H. Takesue, *A Monolithically Integrated Polarization Entangled Photon Pair Source on a Silicon Chip*, Sci. Rep. **2**, 817 (2012).

[37] M. Davanco, J. R. Ong, A. Bahgat Shehata, A. Tosi, I. Agha, S. Assefa, F. Xia, W. M. J. Green, S. Mookherjea, and K. Srinivasan, *Telecommunications-Band Heralded Single Photons from a Silicon Nanophotonic Chip*, Appl. Phys. Lett. **100**, 261104 (2012).

[38] L. Olislager, J. Safioui, S. Clemmen, K. P. Huy, W. Bogaerts, R. Baets, P. Emplit, and S. Massar, *Silicon-on-Insulator Integrated Source of Polarization-Entangled Photons*, Opt. Lett. **38**, 1960 (2013).

[39] A. Orieux, A. Eckstein, A. Lemaitre, P. Filloux, I. Favero, G. Leo, T. Coudreau, A. Keller, P. Milman, and S. Ducci, *Direct Bell States Generation on a III-V Semiconductor Chip at Room Temperature*, Phys. Rev. Lett. **110**, 160502 (2013).

[40] H. Takesue, N. Matsuda, E. Kuramochi, and M. Notomi, *Entangled Photons from On-Chip Slow Light*, Sci. Rep. **4**, 3913 (2014).

[41] A. Politi, J. C. F. Matthews, and J. L. O'Brien, *Shor's Quantum Factoring Algorithm on a Photonic Chip*, Science **325**, 1221 (2009).

[42] J. C. F. Matthews, A. Politi, A. Stefanov, and J. L. O'Brien, *Manipulation of Multiphoton Entanglement in Waveguide Quantum Circuits*, Nat. Photonics **3**, 346 (2009).

[43] A. Crespi, R. Ramponi, R. Osellame, L. Sansoni, I. Bongioanni, F. Sciarrino, G. Vallone, and P. Mataloni, *Integrated Photonic Quantum Gates for Polarization Qubits*, Nat. Commun. **2**, 566 (2011).

[44] P. J. Shadbolt, M. R. Verde, A. Peruzzo, A. Politi, A. Laing, M. Lobino, J. C. F. Matthews, M. G. Thompson, and J. L. O'Brien, *Generating, Manipulating and Measuring Entanglement and Mixture with a Reconfigurable Photonic Circuit*, Nat. Photonics **6**, 45 (2012).

[45] D. Bonneau, E. Engin, K. Ohira, N. Suzuki, H. Yoshida, N. Iizuka, M. Ezaki, C. M. Natarajan, M. G. Tanner, R. H. Hadfield, S. N. Dorenbos, V. Zwiller, J. L. O'Brien, and M. G. Thompson, *Quantum Interference and Manipulation of Entanglement in Silicon Wire Waveguide Quantum Circuits*, New J. Phys. **14**, 045003 (2012).

[46] B. J. Metcalf, N. Thomas-Peter, J. B. Spring, D. Kundys, M. A. Broome, P. C. Humphreys, X.-M. Jin, M. Barbieri, W. S. Kolthammer, J. C. Gates, B. J. Smith, N. K. Langford, P. G. R. Smith, and I. A. Walmsley, *Multiphoton Quantum Interference in a Multiport Integrated Photonic Device*, Nat. Commun. **4**, 1356 (2013).

[47] F. Najafi, J. Mower, N. Harris, F. Bellei, A. Dane, C. Lee, P. Kharel, F. Marsili, S. Assefa, K. K. Berggren, and D. Englund, *On-Chip Detection of Entangled Photons by Scalable Integration of Single-Photon Detectors*, arXiv:1405.4244v1.

[48] C. Schuck, W. H. P. Pernice, and H. X. Tang, *NbTiN Superconducting Nanowire Detectors for Visible and Telecom Wavelengths Single Photon Counting on* Si_3N_4 *Photonic Circuits*, Appl. Phys. Lett. **102**, 051101 (2013).

[49] R. H. Hadfield, *Single-Photon Detectors for Optical Quantum Information Applications*, Nat. Photonics **3**, 696 (2009).

[50] W. H. P. Pernice, C. Schuck, O. Minaeva, and M. Li, *High-Speed and High-Efficiency Travelling Wave Single-Photon Detectors Embedded in Nanophotonic Circuits*, Nat. Commun. **3**, 1325 (2012).

[51] D. Sahin, A. Gaggero, T. B. Hoang, G. Frucci, F. Mattioli, R. Leoni, J. Beetz, M. Lermer, M. Kamp, S. Höfling, and A. Fiore, *Integrated Autocorrelator Based on Superconducting Nanowires*, Opt. Express **21**, 11162 (2013).

[52] J. P. Sprengers, A. Gaggero, D. Sahin, S. Jahanmirinejad, G. Frucci, F. Mattioli, R. Leoni, J. Beetz, M. Lermer, M. Kamp, S. Höfling, R. Sanjines, and A. Fiore, *Waveguide Superconducting Single-Photon Detectors for Integrated Quantum Photonic Circuits*, Appl. Phys. Lett. **99**, 181110 (2011).

[53] C. H. Bennett, G. Brassard *et al.*, in *Proceedings of the IEEE International Conference on Computers, Systems and Signal Processing* (IEEE, New York, 1984), Vol. 175.

[54] N. Gisin, G. Ribordy, W. Tittel, and H. Zbinden, *Quantum Cryptography*, Rev. Mod. Phys. **74**, 145 (2002).

[55] A. K. Ekert, *Quantum Cryptography Based on Bell's Theorem*, Phys. Rev. Lett. **67**, 661 (1991).

[56] C. Branciard, N. Gisin, B. Kraus, and V. Scarani, *Security of Two Quantum Cryptography Protocols Using the Same Four Qubit States*, Phys. Rev. A **72**, 032301 (2005).

[57] R. Renner, N. Gisin, and B. Kraus, *Information-Theoretic Security Proof for Quantum-Key-Distribution Protocols*, Phys. Rev. A **72**, 012332 (2005).

[58] G. Brassard, N. Lütkenhaus, T. Mor, and B. C. Sanders, *Limitations on Practical Quantum Cryptography*, Phys. Rev. Lett. **85**, 1330 (2000).

[59] M. Curty, M. Lewenstein, and N. Lütkenhaus, *Entanglement as a Precondition for Secure Quantum Key Distribution*, Phys. Rev. Lett. **92**, 217903 (2004).

[60] D. Deutsch, A. Ekert, R. Jozsa, C. Macchiavello, S. Popescu, and A. Sanpera, *Quantum Privacy Amplification and the Security of Quantum Cryptography over Noisy Channels*, Phys. Rev. Lett. **77**, 2818 (1996).

[61] I. Marcikic, H. de Riedmatten, W. Tittel, H. Zbinden, M. Legré, and N. Gisin, *Distribution of Time-Bin Entangled Qubits over 50 km of Optical Fiber*, Phys. Rev. Lett. **93**, 180502 (2004).

[62] C. H. Bennett, G. Brassard, C. Crépeau, and U. M. Maurer, *Generalized Privacy Amplification*, IEEE Trans. Inf. Theory **41**, 1915 (1995).

[63] J. Mower, Z. Zhang, P. Desjardins, C. Lee, J. H. Shapiro, andD. Englund, *High-Dimensional Quantum Key Distribution Using Dispersive Optics*, Phys. Rev. A **87**, 062322 (2013).

[64] M. A. Broome, A. Fedrizzi, S. Rahimi-Keshari, J. Dove, S. Aaronson, T. C. Ralph, and A. G. White, *Photonic Boson Sampling in a Tunable Circuit*, Science **339**, 794 (2013).

[65] A. M. Childs, D. Gosset, and Z. Webb, *Universal Computation by Multiparticle Quantum Walk*, Science **339**, 791 (2013).

[66] A. Crespi, R. Osellame, R. Ramponi, D. J. Brod, E. F. Galvao, N. Spagnolo, C. Vitelli, E. Maiorino, P. Mataloni, and F. Sciarrino, *Integrated Multimode Interferometers with Arbitrary Designs for Photonic Boson Sampling*, Nat. Photonics **7**, 545 (2013).

[67] M. Tillmann, B. Dakic, R. Heilmann, S. Nolte, A. Szameit, and P. Walther, *Experimental Boson Sampling*, Nat. Photonics **7**, 540 (2013).

[68] N. Spagnolo, C. Vitelli, M. Bentivegna, D. J. Brod, A. Crespi, F. Flamini, S. Giacomini, G. Milani, R. Ramponi, P. Mataloni, R. Osellame, E. F. Galvao, and F. Sciarrino, *Experimental Validation of Photonic Boson Sampling*, Nat. Photonics **8**, 615 (2014).

[69] M. A. Nielsen and I. L. Chuang, *Quantum Computation and Quantum Information*, 1st ed., Cambridge Series on Information and the Natural Sciences(Cambridge University Press, Cambridge, England, 2004).

[70] D. Gottesman and I. L. Chuang, *Demonstrating the Viability of Universal Quantum Computation Using Teleportation and Single-Qubit Operations*, Nature (London) **402**, 390 (1999).

[71] E. Knill, R. Laflamme, and G. J. Milburn, *A Scheme for Efficient Quantum Computation with Linear Optics*, Nature (London) **409**, 46 (2001).

[72] R. Jozsa and N. Linden, *On the Role of Entanglement in Quantum-Computational Speed-Up*, Proc. R. Soc. A **459**, 2011 (2003).

[73] W.-B. Gao, A. M. Goebel, C.-Y. Lu, H.-N. Dai, C. Wagenknecht, Q. Zhang, B. Zhao, C.-Z. Peng, Z.-B. Chen, Y.-A. Chen, and J.-W. Pan, *Teleportation-Based Realization of an Optical Quantum Two-Qubit Entangling Gate*, Proc. Natl. Acad. Sci. U.S.A. **107**, 20869 (2010).

[74] T. D. Ladd, F. Jelezko, R. Laflamme, Y. Nakamura, C. Monroe, and J. L. O'Brien, *Quantum Computers*, Nature (London) **464**, 45 (2010).

[75] L. G. Helt, Z. Yang, M. Liscidini, and J. E. Sipe, *Spontaneous Four-Wave Mixing in Microring Resonators*, Opt. Lett. **35**, 3006 (2010).

[76] L. He, Yang Liu, C. Galland, A. E. J. Lim, G.-Q. Lo, T. Baehr-Jones, and M. Hochberg, *A High-Efficiency Nonuniform Grating Coupler Realized with 248-nm Optical Lithography*, IEEE Photonics Technol. Lett. **25**, 1358 (2013).

[77] T. Baehr-Jones, R. Ding, A. Ayazi, T. Pinguet, M. Streshinsky, N. Harris, J. Li, L. He, M. Gould, Y. Zhang *et al.*, *A* 25 Gb/s *Silicon Photonics Platform*, arXiv:1203.0767.

[78] N. C. Harris, Y. Ma, J. Mower, T. Baehr-Jones, D. Englund, M. Hochberg, and C. Galland, *Efficient, Compact and Low Loss Thermo-optic Phase Shifter in Silicon*, Opt. Express **22**, 10487 (2014).

[79] G. Fujii, N. Namekata, M. Motoya, S. Kurimura, and S. Inoue, *Bright Narrowband Source of Photon Pairs at Optical Telecommunication Wavelengths Using a Type-II Periodically Poled Lithium Niobate Waveguide*, Opt. Express **15**, 12769 (2007).

[80] H. Takesue and K. Shimizu, *Effects of Multiple Pairs on Visibility Measurements of Entangled Photons Generated by Spontaneous Parametric Processes*, Opt. Commun. **283**, 276 (2010).

[81] Y. Zhang, S. Yang, A. E.-J. Lim, G.-Q. Lo, C. Galland, T. Baehr-Jones, and M. Hochberg, *A Compact and Low Loss Y-Junction for Submicron Silicon Waveguide*, Opt. Express **21**, 1310 (2013).

[82] C. A. Husko, A. S. Clark, M. J. Collins, A. De Rossi, S. Combrié, G. Lehoucq, I. H. Rey, T. F. Krauss, C. Xiong, and B. J. Eggleton, *Multi-photon Absorption Limits to Heralded Single Photon Sources*, Sci. Rep. **3**, 3087 (2013).

[83] M. Varnava, D. E. Browne, and T. Rudolph,, *How Good Must Single Photon Sources and Detectors Be for Efficient Linear Optical Quantum Computation?*, Phys. Rev. Lett. **100**, 060502 (2008).

[84] A. L. Migdall, D. Branning, and S. Castelletto, *Tailoring Single-Photon and Multiphoton Probabilities of a Single-Photon On-Demand Source*, Phys. Rev. A **66**, 053805 (2002).

[85] J. Mower and D. Englund, *Efficient Generation of Single and Entangled Photons on a Silicon Photonic Integrated Chip*, Phys. Rev. A **84**, 052326 (2011).

[86] A. P. Lund, S. Rahimi-Keshari, and T. C. Ralph, *Boson Sampling from Gaussian States*, Phys. Rev. Lett. **113**, 100502 (2014).

[87] D. Grassani, S. Azzini, M. Liscidini, M. Galli, M. J. Strain, M. Sorel, J. E. Sipe, and D. Bajoni, *A Micrometer-Scale Integrated Silicon Source of Time-Energy Entangled Photons*, arXiv:1409.4881.

[88] Z. Zhang, J. Mower, D. Englund, F. N. C. Wong, and J. H. Shapiro, *Unconditional Security of Time-Energy Entanglement Quantum Key Distribution Using Dual-Basis Interferometry*, Phys. Rev. Lett. **112**, 120506 (2014).